Available online at www.sciencedirect.com
SCIENCE DIRECT®
Journal of Solid State Chemistry 177 (2004) 3715–3720
JOURNAL OF SOLID STATE CHEMISTRY
www.elsevier.com/locate/jssc

High-pressure dissociation of silver mercury iodide, Ag_2HgI_4

D.C. Parfitt[a], S. Hull[b,*], D.A. Keen[a,b], W. Crichton[c]

[a]*Department of Physics, Oxford University, Parks Road, Oxford OX1 3PU, UK*
[b]*The ISIS Facility, Rutherford Appleton Laboratory, Chilton, Didcot, OX11 0QX, UK*
[c]*ESRF, 6 Rue Jules Horowitz, BP 220, 38043 Grenoble CEDEX 9, France*

Received 5 May 2004; received in revised form 21 June 2004; accepted 24 June 2004
Available online 25 August 2004

Abstract

High-pressure X-ray diffraction has been used to probe the behavior of the superionic conductor silver mercury iodide (Ag_2HgI_4) at pressures up to 5 GPa and at temperatures from 295 to 370 K. Significant changes in the diffraction spectra, indicative of structural transitions, are observed around 0.7 and 1.3 GPa across the range of temperatures studied. The change at 0.7 GPa is shown to correspond to the dissociation of silver mercury iodide into silver iodide and mercury iodide, i.e., $Ag_2HgI_4 \rightarrow 2AgI + HgI_2$. The second transition, at 1.3 GPa, is due to a structural phase transition within HgI_2. Rietveld analysis of the diffraction data is used to confirm and refine all the known crystal structures.

Keywords: Superionic conduction; Silver mercury iodide; High-pressures; X-ray diffraction; Dissociation

1. Introduction

Silver mercury iodide, Ag_2HgI_4, adopts a number of different structural phases within a modest range of temperatures and pressures, several of which are superionic phases characterized by high ionic conductivities (for a summary of the literature, see Refs. [1,2] and references therein). The structure of the β phase of Ag_2HgI_4 stable under ambient conditions, which is not superionic, is tetragonal and assigned to space group $I\bar{4}$ [1]. The iodine atoms adopt a slightly distorted face centered cubic (f.c.c.) arrangement and the cations occupy $\frac{3}{8}$ of the tetrahedrally co-ordinated positions, in an ordered manner derived from the chalcopyrite ($A_2B_2X_4$) structure by the addition of cation vacancies. Upon heating, the first superionic α phase appears at 325 K and the transition is classified as type I in the nomenclature of Boyce and Huberman [3]. The structure of α-Ag_2HgI_4 is similar to that of the β phase, except that the iodine sublattice is now an ideal f.c.c. arrangement and diffraction studies show the cations to be disordered over half of the tetrahedrally co-ordinated positions [1]. Crystallographically, α-Ag_2HgI_4 is described in the cubic space group $F\bar{4}3m$, with each cation site having an average occupancy of $\frac{1}{2} \times Ag^+$ and $\frac{1}{4} \times Hg^{2+}$. Further, high-temperature transitions have been observed at 410 and ~445 K, to superionic phases labelled δ and ε characterized by hexagonal close packed and body centered cubic iodine sublattices, respectively [2].

Several studies have investigated the behavior of Ag_2HgI_4 under pressure [4–8]. These have concentrated on establishing the phase boundaries within Ag_2HgI_4 by probing the macroscopic properties of the material and have provided little insight into the structures of the discovered phases. Unfortunately, issues such as sample purity and pressure calibration have tended to yield rather inconclusive and/or conflicting results. The most complete study was carried out by Baranowski et al. [8], in which the phase diagram of Ag_2HgI_4 was mapped out up to 450 K and 1 GPa using the differential scanning calorimetry technique (see Fig. 1). The phase boundaries of the α, β and δ phases were clearly determined, as was

*Corresponding author. Fax: +44-1235-445720.
E-mail address: s.hull@rl.ac.uk (S. Hull).

0022-4596/$ - see front matter © 2004 Elsevier Inc. All rights reserved.
doi:10.1016/j.jssc.2004.06.039

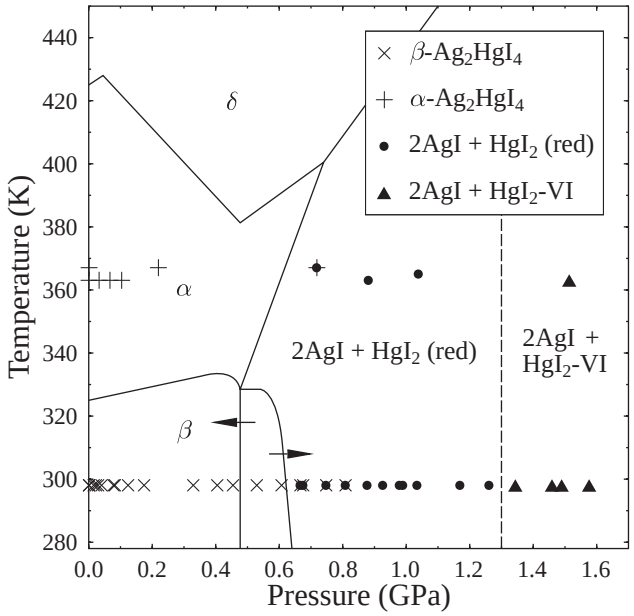

Fig. 1. Pressure–temperature phase diagram of Ag_2HgI_4 showing the phase boundaries (—) determined in Ref. [8] up to 1 GPa. The lines at ~0.5 and ~0.6 GPa are annotated with arrows corresponding to decreasing and increasing pressure, respectively. The individual markers represent the phases observed by the current authors within the diffraction data and are explained in the key. The dashed line at 1.3 GPa represents the approximate pressure of the transition from the ambient (red) to the high-pressure phase (VI) within HgI_2 which is assumed, in the absence of evidence to the contrary, to be independent of pressure.

the existence of a high-pressure (γ) phase at pressures above 0.6 GPa. A phase transition occurring between 0.3 and 0.4 GPa reported in many of the previous studies was attributed to the pressure-induced transition to the rocksalt-structured phase (AgI-III) within AgI present as an impurity in the Ag_2HgI_4 samples [9]. Raman spectroscopy studies showed that the Hg–I bond vibration frequency is lowered on transforming from the β to the γ phase [6]; an observation consistent with the Hg^{2+} ion moving from a tetrahedral anion environment within the β phase to an octahedrally co-ordinated one within the γ-phase. This led to the suggestion that the γ phase of Ag_2HgI_4 may possess a rocksalt-like structure, similar to the high-pressure phase III observed within its parent binary compound AgI [10]. If the high-pressure forms of AgI and Ag_2HgI_4 have related crystal structures, then it follows that the cations within γ-Ag_2HgI_4 may also become disordered upon heating, in a manner analogous to the gradual (type-II [3]) superionic transition within rocksalt-structured AgI-III [11].

Studies of Ag_2HgI_4 at pressures above ~1 GPa are fragmentary and incomplete. Webb et al. [5] took anomalies in the electrical conductivity as indicative of phase transitions and, as in previous studies, transitions were found at 0.4 GPa (due to the phase transition within an AgI impurity) and 0.6 GPa (the $\beta \rightarrow \gamma$ transition in Ag_2HgI_4). Transitions were also observed at 0.75, 4.4 and 7.5 GPa. By contrast, Kamigaki et al. [7], reported transitions at 0.8, 2.0 and 3.6 GPa using a combination of optical observation and differential thermal analysis.

The purpose of this paper is, therefore, to present the results of a series of X-ray powder diffraction measurements carried out over a range of temperatures from 295 to 370 K and at pressures up to 5 GPa. The aims are (i) to confirm the phase designations proposed by Baranowski et al. [8]; (ii) to deduce the structure of the high-pressure γ phase of Ag_2HgI_4; (iii) to search for evidence of cation disorder within the γ phase on increasing temperature; and (iv) to confirm the presence of any further phase transitions within Ag_2HgI_4 at higher pressures.

2. Experimental method

X-ray diffraction spectra were taken using the ID30 high-pressure beamline at the European Synchrotron Radiation Facility, Grenoble, France. Samples of Ag_2HgI_4 were obtained from the Cerac Chemical Company with a stated purity of 99.5%. The sample was first finely ground, to ensure a good degree of powder averaging, and then loaded into a boron nitride (BN) container. The container was surrounded by a graphite sheath, which formed part of the heating circuit, and then by a boron epoxy resin gasket. The outside diameters of the sample, BN container and graphite sheath were approximately 1, 3 and 3.5 mm, respectively. Heating of the cell was achieved by passing an electrical current through the graphite cylinder surrounding the inner BN container. The temperature of the sample was monitored using a type-K thermocouple mounted in the side of the pressure cell which penetrated into the inner BN canister.

During the diffraction experiment, the sample was illuminated by a 100 μm wide × 300 μm high monochromatic X-ray beam of wavelength $\lambda = 0.15816$ Å. Diffracted photons were collected using a MAR345 image plate and the images corrected for geometric distortions using the Fit2D program [12]. The Debye–Scherrer rings were observed to be circular with an even distribution of diffracted intensity, indicating a good degree of powder averaging. The images were then integrated around circular annuli [13] to produce a diffraction spectrum as a function of scattering angle, 2θ. The distance between the sample and detector was calibrated using the literature values of the unit cell of Ag_2HgI_4 at ambient pressure and temperature [1]. At each pressure–temperature data point an additional spectrum was taken with the X-ray beam grazing the edge of the sample

rather than passing through its center. This second spectra, dominated by scattering from the BN immediately surrounding the sample, was fitted using the literature structure of hexagonal BN [14]. The refined values of the BN unit cell and the temperature measured by the thermocouple were then used with the published equation of state of BN [15] to derive the pressure in the sample.

The sample spectra were fitted using the GSAS Rietveld refinement program [16]. The least-squares refinement for each phase of known structure used an overall scale factor, four peak profile coefficients, the lattice parameters, plus the atomic co-ordinates and isotropic atomic displacement factor for each occupied symmetry position. An eight parameter shifted Chebyschev function was also used to describe the background scattering. For those diffraction spectra containing phases with incomplete structural models, a 'le Bail' fit was used [17]. In this technique the intensity of each Bragg reflection is refined independently until the best fit to the data is obtained. Whilst a 'le Bail' fit provides no structural information, it is useful in testing the validity of the space group assignment and in refining the unit cell dimensions.

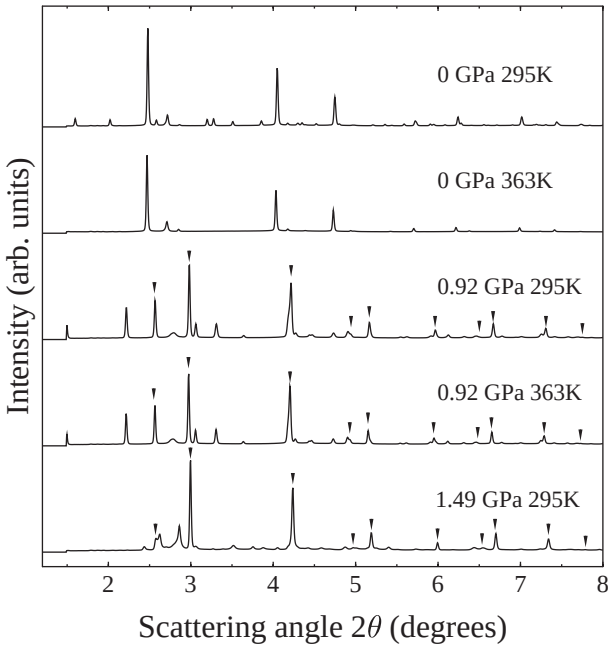

Fig. 2. Representative diffraction spectra taken at the various temperatures and pressures indicated. The small relatively broad peak at $2\theta \sim 2.8^\circ$ is due to scattering from the BN sample container. Note the persistence of the rocksalt-structured AgI peaks (marked with arrow heads) in the bottom three plots.

3. Results and discussion

The pressure–temperature points at which each spectrum was measured are shown in Fig. 1. Two runs were made: the first recorded diffraction data at a number of pressure points up to 5 GPa, and the second probed the region around the $\beta \rightarrow \gamma$ transition in more detail. Representative examples of the diffraction spectra are shown in Fig. 2.

The structures of the β and α phases of Ag_2HgI_4 from Ref. [1] were used to analyze the room pressure diffraction data collected at 295 and 367 K, respectively. An excellent fit was obtained to both data sets and the refined parameters are presented in Table 1. Upon applying pressure, two major structural transitions were observed as abrupt changes in the measured diffraction spectra. The first transition began at 0.6 GPa and had reached completion by 0.8 GPa; the second transition was rather sharper and occurred between 1.25 and 1.35 GPa. In the region between 0.8 and 1.25 GPa, the observed peaks were consistent with the structures of the high-pressure rocksalt-structured phase of AgI (AgI-III) [10,11] and the ambient pressure (red) phase of HgI_2 [18,19] (Table 2). The first transition is, therefore, attributed to the pressure-induced dissociation of Ag_2HgI_4, i.e., $Ag_2HgI_4 \rightarrow 2AgI + HgI_2$.

Having identified the diffraction peaks arising from rocksalt-structured AgI-III in the spectra above the first transition (marked in Fig. 2), it is clear that they are also present above the second transition occurring at 1.3 GPa. The observed changes in the diffraction spectra at this pressure are, therefore, solely due to a structural transition within HgI_2. Unfortunately, at pressures above 1.3 GPa the diffraction peaks due to this new phase of HgI_2 became very broad, limiting the structural information that could be extracted. Hostettler et al. [20] have conducted an X-ray diffraction study of HgI_2 at high pressures and identified a new phase that exists above 1.3 GPa. This phase was suggested to possess a similar structure to that of the 'yellow' phase stable at high temperatures, with a monoclinic structure characterized by layers of I–Hg–I dimers [20]. It is referred to here as HgI_2-VI, to avoid confusion with the two other 'yellow' polymorphs of HgI_2 [19,20]. Fig. 3 (ii) shows a 'le Bail' fit to the diffraction data collected at 1.3 GPa, using the proposed monoclinic unit cell for HgI_2-VI [20]. Whilst this structural model (Table 2) correctly reproduces the observed peak positions and possesses systematic absences consistent with the proposed $P2_1/a$ space group [20], the broadness of the peak profiles and the low symmetry of the unit cell prevent an unambiguous confirmation or, indeed, the determination of the full structure.

The ambient temperature unit cell volumes of Ag_2HgI_4, AgI and both forms of HgI_2 are plotted as a function of pressure in Fig. 4. Also shown is the relative change in sample volume calculated as the sum of the rocksalt-structured AgI-III and 'red' HgI_2 unit cell volumes (in the pressure range 0.6–1.3 GPa), or the unit cell volume of rocksalt-structured AgI-III plus half the

Table 1
Summary of the structural properties of the α and β phases of Ag_2HgI_4 at ambient pressure determined by Rietveld refinement of the powder X-ray diffraction data

Phase	β-Ag_2HgI_4	α-Ag_2HgI_4
Space group	$I\bar{4}$	$F\bar{4}3m$
Temperature (K)	295	367
Lattice parameters	$a = 6.31934(12)$ Å $c = 12.6050(4)$ Å $c/a = 1.9946(6)$	$a = 6.33844(10)$ Å
Formula units per unit cell	$Z = 2$	$Z = 1$
Unit cell volume (Å^3)	503.372(22)	254.652(7)
I^-	8(*g*) at x_I, y_I, z_I, etc. $x_I = 0.2675(6)$ $y_I = 0.2294(6)$ $z_I = 0.13264(27)$ $B_I = 2.88(5)$Å^2	4(*c*) at $\frac{1}{4}$, $\frac{1}{4}$, $\frac{1}{4}$, etc. $B_I = 5.11(6)$ Å^2
Hg^{2+}	2(*a*) at 0,0,0, etc. $B_{Hg} = 4.34(10)$Å^2	4(*a*) at 0,0,0, etc. $B_{Hg} = B_{Ag} = 9.04(13)$ Å^2 Occupancy $= \frac{1}{4}$
Ag^+	Ag1 in 2(*b*) at 0,0,$\frac{1}{2}$, etc. $B_{Ag1} = 4.6(2)$ Å^2 Ag2 in 2(*c*) at 0, $\frac{1}{2}$, $\frac{1}{4}$, etc. $B_{Ag2} = 5.5(2)$ Å^2	4(*a*) at 0,0,0, etc. $B_{Ag} = B_{Hg} = 9.04(13)$ Å^2 Occupancy $= \frac{1}{2}$
Fit details	$N_D = 1740$ $N_P = 442$ $N_V = 24$ $R_P = 0.069$ $R_{WP} = 0.096$ $R_{EXP} = 0.100$	$N_D = 1740$ $N_P = 88$ $N_V = 21$ $R_P = 0.060$ $R_{WP} = 0.081$ $R_{EXP} = 0.102$

The *B* values are the refined isotropic thermal vibration parameters. The profile (P), weighted profile (WP) and expected weighted profile (EXP) *R*-factors are given by

$$R_p^2 = \sum_{N_D}(I_{obs} - I_{calc})^2 \Big/ \sum_{N_D}(I_{obs})^2,$$

$$R_{WP}^2 = \sum_{N_D}\frac{(I_{obs} - I_{calc})^2}{(\sigma I_{obs})^2} \Big/ \sum_{N_D}\frac{(I_{obs})^2}{(\sigma I_{obs})^2},$$

and

$$R_{EXP}^2 = (N_D - N_V) \Big/ \sum_{N_D}\frac{(I_{obs})^2}{(\sigma I_{obs})^2},$$

respectively [16]. The summations are made over the N_D data points used in the fit. I_{obs} and I_{calc} are the observed and calculated intensities, respectively, and σI_{obs} is the estimated standard deviation on I_{obs} derived from the counting statistics. N_V is the number of fitted variables and N_P is the number of Bragg peaks within the fitted data range.

unit cell volume of HgI_2-VI (pressures greater than 1.3 GPa). This takes into account the differing number of formula units within each unit cell and that two AgI units are produced in the pressure-induced dissociation of Ag_2HgI_4 (Table 2). The volume change associated with the dissociation of Ag_2HgI_4 into $2AgI + HgI_2$ (red) is $\approx 7.4\%$.

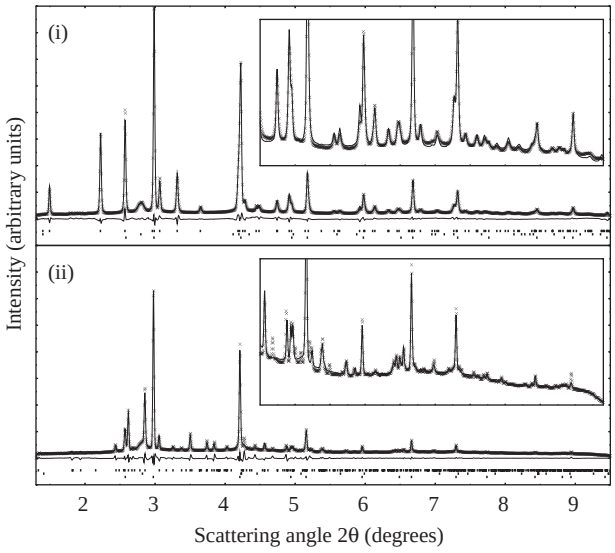

Fig. 3. Plots showing the fit to the diffraction data collected at (i) 0.8 GPa and (ii) 1.3 GPa at ambient temperature. In both cases the experimental intensities are shown as crosses and the solid lines are the fits to the data. The difference profiles are shown as lines under each plot. Plot (i) uses the structural models for 'red' HgI_2 (upper tick-marks), hexagonal BN (middle tick-marks) and rocksalt-structured AgI-III (lower tick-marks); plot (ii) is a 'le Bail' refinement using the cell parameters from HgI_2-VI (upper tick-marks), hexagonal BN (middle tick-marks) and rocksalt-structured AgI-III (lower tick-marks). Insets show a magnified portion of the data. The only significant contribution to the spectra from hexagonal BN is due to the (002) peak at $2\theta \sim 2.8$.

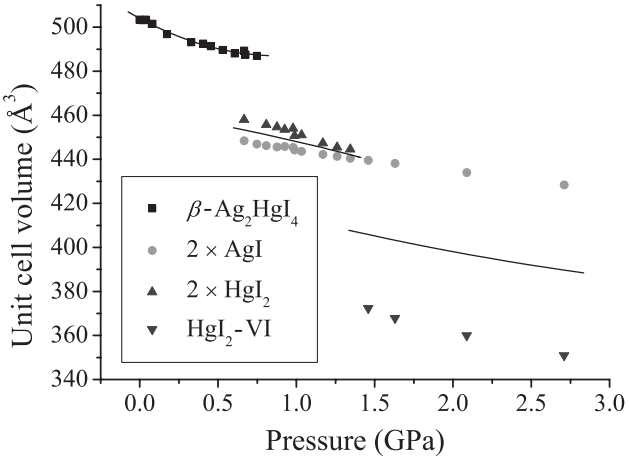

Fig. 4. The variation of unit cell volumes as a function of pressure. The plotted points represent the experimentally determined values of the lattice parameters for the four different phases encountered. The values for rocksalt-structured AgI-III and 'red'-HgI_2 have been multiplied by a factor of 2 to bring them onto a comparable scale. Smooth lines represent a fit to the total sample volume calculated as the sum of the rocksalt-structured AgI-III and 'red' HgI_2 unit cell volumes (in the pressure range 0.6–1.3 GPa), or the unit cell volume of rocksalt-structured AgI-III plus half the unit cell volume of HgI_2-VI (pressures greater than 1.3 GPa). This takes into account the differing number of formula units within each unit cell and that two AgI units are produced in the pressure-induced dissociation of Ag_2HgI_4.

Table 2
Summary of the structural properties of the two phases of HgI_2 after pressure-induced dissociation of Ag_2HgI_4 determined by least-squares refinement of the powder X-ray diffraction data

Phase	'Red' HgI_2	HgI_2-VI (high-pressure yellow phase)
Space group	$P4_2/nmc$	$P2_1/a$
Temperature (K)	295	295
Pressure (GPa)	1.1	1.6
Lattice parameters	$A = 4.31617(18)$ Å $C = 12.0875(10)$ Å $C/a = 2.8005(3)$	$a = 13.9574(15)$ Å $b = 5.4009(6)$ Å $c = 5.1057(6)$ Å
Formula units per unit cell	$Z = 2$	$Z = 4$
Unit cell volume (Å^3)	225.182(23)	368.75(8)
I^-	4(d) at $\frac{1}{4}, \frac{1}{4}, z_I$, etc. $z_I = 0.3926(3)$ $B_I = 3.30(9)$ Å^2	'Le-Bail fit' No structural information
Hg^{2+}	2(a) at $\frac{1}{4}, \frac{1}{4}, \frac{3}{4}$, etc. $B_{Hg} = 3.77(9)$ Å^2	
Fit details	$N_D = 1843$ $N_P = 310$ $N_V = 28$ $R_P = 0.061$ $R_{WP} = 0.083$ $R_{EXP} = 0.116$	$N_D = 1792$ $N_V = 33$ $R_P = 0.072$ $R_{WP} = 0.114$ $R_{EXP} = 0.113$

The B values are the refined isotropic thermal vibration parameters. The profile (P), weighted profile (WP) and expected weighted profile (EXP) R-factors are given by

$$R_P^2 = \sum\nolimits_{N_D} (I_{obs} - I_{calc})^2 \Big/ \sum\nolimits_{N_D} (I_{obs})^2,$$

$$R_{WP}^2 = \sum_{N_D} \frac{(I_{obs} - I_{calc})^2}{(\sigma I_{obs})^2} \Big/ \sum_{N_D} \frac{(I_{obs})^2}{(\sigma I_{obs})^2},$$

and

$$R_{EXP}^2 = (N_D - N_V) \Big/ \sum_{N_D} \frac{(I_{obs})^2}{(\sigma I_{obs})^2},$$

respectively [16]. The summations are made over the N_D data points used in the fit. I_{obs} and I_{calc} are the observed and calculated intensities, respectively, and σI_{obs} is the estimated standard deviation on I_{obs} derived from the counting statistics. N_V is the number of fitted variables and N_P is the number of Bragg peaks within the fitted data range.

Upon returning to ambient conditions after pressurization, the measured diffraction spectra were consistent with a sample containing 'red' HgI_2, the original β-phase of Ag_2HgI_4 and the zincblende-structured (γ) phase of AgI. No significant intensity was observed at the expected Bragg peak positions for wurtzite-structured β-AgI (which is also a stable form at room temperature and pressure [21]) and this phase was not included in the refinement. Fractions of the refined phases by percent weight were Ag_2HgI_4—46(1) %, HgI_2—27(1) % and γ-AgI—27(1) %. The pressure-induced dissociation of Ag_2HgI_4 is, therefore, at least partially reversible.

3.1. Comparison with previous literature results

The behavior of Ag_2HgI_4 at relatively low pressures was discussed in Section 1, with the reported phase transitions observed between 0.3 and 0.4 GPa attributed to the presence of AgI as an impurity within the prepared samples [8,9]. The transition in Ag_2HgI_4 observed at 0.6–0.8 GPa is reported in nearly all previous studies and has been shown here to be due to the pressure-induced dissociation of Ag_2HgI_4 into AgI and HgI_2. This observation may also explain the large hysteresis between increasing and decreasing pressure conditions shown in the phase diagram of Baranowski et al. [8]. The lowering of the frequency of the Hg–I Raman mode of Ag_2HgI_4 with increasing pressure through the transition at 0.6–0.8 GPa was previously attributed to a change in the mercury ion's anion environment from 4- to 6-fold co-ordination [4,7,8]. A comparison of the Raman peaks from Refs. [22,23] and [24,25] shows that the Raman spectra of Ag_2HgI_4 collected at high pressure and of 'red' HgI_2 are almost identical, consistent with the dissociation of Ag_2HgI_4 reported here.

After the structural transition within HgI_2 observed at 1.3 GPa, no further transitions were observed in this experiment on increasing pressure up to 5 GPa at room temperature. On the basis of published studies, additional phase transitions are expected in HgI_2 at 8.3 GPa [20] and in AgI at 11.3 GPa [26]. It is possible that the former corresponds to the transition reported previously in Ag_2HgI_4 at 7.5 GPa [6], but the origins of the other observed high-pressure transitions remain unclear. Hostettler et al. [20] have shown the existence of seven different polymorphs of HgI_2 within a relatively modest range of temperatures and pressures and several of the reported transitions within Ag_2HgI_4 at pressures greater than 1 GPa may, in fact, be occurring within HgI_2.

Finally, it is interesting to note that Ag_2HgI_4 also has a copper analogue. Cu_2HgI_4 possesses a closely related structure under ambient conditions, but a different ordered arrangement of the cations over the tetrahedrally co-ordinated sites leads to $I\bar{4}2m$ symmetry rather than $I\bar{4}$ [1]. X-ray diffraction studies of Cu_2HgI_4 report the presence of a transition at ~7 GPa on increasing pressure, to a phase with a hexagonal structure with $a = 8.28(2)$ Å and $c = 3.40(1)$ Å and space group $P\bar{3}1m$ [27]. However, the reported structural model is probably in error, since it contains anomalously short I^-–I^- contacts. More detailed X-ray diffraction studies are required to investigate whether Cu_2HgI_4 also undergoes pressure-induced dissociation, since CuI itself shows extensive polymorphism at relatively low pressures [28].

4. Conclusions

The purpose of this paper is to explain the structural behavior of silver mercury iodide, Ag_2HgI_4, at high pressures and temperatures using in situ X-ray powder diffraction. The experimental results are consistent with the phase diagram reported by Baranowski et al. [8], though the high-pressure γ phase is, in fact, a two-phase mixture of AgI and HgI_2. With this interpretation, some progress can be made to resolve the discrepancies between the results reported in several previous publications. The high-pressure behavior of HgI_2 is itself an interesting topic, though not directly the subject of the current paper. Clearly, further work is needed to confirm the structure of the high-pressure phase HgI_2-VI, with the emphasis on obtaining good-quality high-pressure diffraction data.

Acknowledgments

We would like to express our gratitude to Matt Tucker, Adrian Barnes and Mohammed Mezouar for their assistance with the experimental diffraction work and to Marc Hostettler and his colleagues for providing their unpublished data on the high-pressure structural behavior of HgI_2. Two of the authors (DCP and DAK) would like to thank the Engineering and Physical Sciences Research Council for financial support. We are also indebted to the European Synchrotron Radiation Facility for their provision of beam time on beamline ID30.

References

[1] S. Hull, D.A. Keen, J. Phys.: Condens. Matter 12 (2000) 3751–3765.
[2] S. Hull, D.A. Keen, J. Phys: Condens. Matter 13 (2001) 5597–5610.
[3] J.B. Boyce, B.A. Huberman, Phys. Rep. 51 (1979) 189–265.
[4] J.I. McOmber, D.F. Shriver, M.A. Ratner, J.R. Ferraro, P. la Bonville Walling, J. Phys. Chem. Solids 43 (1982) 903–909.
[5] A.W. Webb, J. Phys. Chem. Solids 34 (1973) 501–508.
[6] R. Weil, A.W. Lawson, J. Chem. Phys. 41 (1964) 832–836.
[7] K. Kamigaki, J. Mizuki, S. Abe, Solid State Ionics 3-4 (1981) 57–60.
[8] B. Baranowski, M. Friesel, A. Lundén, Phys. Rev. B 33 (1986) 7753–7761.
[9] M. Friesel, A. Lundén, B. Baranowski, Phys. Rev. B 32 (1985) 2506–2509.
[10] D.A. Keen, S. Hull, J. Phys.: Condens. Matter 5 (1993) 23–32.
[11] D.A. Keen, S. Hull, W. Hayes, N.J.G. Gardner, Phys. Rev. Lett. 77 (1996) 4914–4917.
[12] A.P. Hammersley, ESRF Internal Report, ESRF98HA01 T V9.129, 1998.
[13] A.P. Hammersley, S.O. Svensson, M. Hanfland, A.N. Fitch, D. Häusermann, High Pressure Res. 14 (1996) 235–248.
[14] Y.N. Xu, W.Y. Ching, Phys. Rev. B 48 (1993) 4335–4351.
[15] Y. le Godec, D. Martinez-Garcia, M. Mezouar, G. Syfosse, J.P. Itie, J.P. Besson, High Pressure Res. 17 (2000) 35–46.
[16] A.C. Larson, R.B. von Dreele, Los Alamos National Laboratory Report LAUR 86-748, 1994.
[17] A. le Bail, H. Duroy, J.L. Fourquet, Mater. Res. Bull. 23 (1988) 447–452.
[18] J.M. Delgado, R.K. McMullan, B.J. Wuensch, Trans. Am. Crystallogr. Assoc. 23 (1987) 93–95.
[19] G.A. Jeffrey, M. Vlasse, Inorg. Chem. 6 (1967) 396–399.
[20] M. Hostettler, H. Birkedal, D. Schwarzenbach, Chimia 55 (2001) 541–545.
[21] G. Burley, J. Chem. Phys. 38 (1963) 2807–2812.
[22] D. Greig, D.F. Shriver, J.R. Ferraro, J. Chem. Phys. 66 (1997) 5248–5250.
[23] D.M. Adams, P.D. Hatton, J. Raman Spectrosc. 14 (1983) 154–161.
[24] M.Y. Khilji, W.F. Sherman, A. Stadtmuller, G.R. Wilkinson, J. Raman Spectrosc. 11 (1981) 238–245.
[25] N. Kuroda, T. Iwabuchi, Y. Nishina, J. Phys. Soc. Japan 52 (1983) 2419–2427.
[26] S. Hull, D.A. Keen, Phys. Rev. B 59 (1999) 750–761.
[27] H. Mikler, Monatsch. Chem. 120 (1989) 7–10.
[28] S. Hull, D.A. Keen, Phys. Rev. B 50 (1994) 5868–5885.